Reviews

g Interaction Parameter of Polymer–Solvent Systems

Rosa M. Masegosa

Departamento de Quimica Fisica, Facultad de Ciencias Quimicas, Universidad Complutense, 28040 Madrid, Spain

Margarita G. Prolongo

Cátedra de Quimica, Escuela Técnica Superior de Ingenieros Aeronaúticos, Universidad Politécnica de Madrid, 28040 Madrid, Spain

Arturo Horta

Departamento de Quimica General y Macromoléculas, Facultad de Ciencias, Universidad a Distancia (UNED), 28040 Madrid, Spain. *Received November 4, 1985*

ABSTRACT: Prediction of thermodynamic properties on ternary systems formed by a polymer and two solvents or two polymers and a solvent requires the knowledge of the parameter $g°$, characteristic of the interaction of the corresponding binary pairs. $g°$ may be calculated from the polymer concentration dependence of the Flory–Huggins parameter, χ, in binary systems. We have calculated $g°$ for 41 polymer–solvent systems for which data of χ vs. concentration were available in the literature. These values of $g°$ have been compared with those calculated from the Flory theory.

The thermodynamic state of a polymer–solvent system is completely determined (at fixed temperature and pressure) by means of the interaction parameter g. This g is defined through the noncombinatorial part of the Gibbs mixing function, ΔG_M (see eq 2). The more usual interaction parameter, χ, is defined similarly but through the solvent chemical potential, $\Delta\mu_1$, derived from ΔG_M (see eq 3).

In ternary systems composed of one polymer and two liquids or of two polymers and one solvent, the total Gibbs mixing function of the system can be written in terms of the g interaction parameters of the corresponding binary pairs, according to the Flory–Huggins formalism.[1] When studying polymers in mixed solvents, it has been customary to introduce an additional interaction parameter, called ternary,[2] g_T. It has been the object of numerous investigations to attempt the prediction of the total sorption and the preferential adsorption of polymers in mixed solvents from the interaction parameters of the binary pairs and use of the ternary parameter as adjustable. This has shown that such a ternary parameter is of great importance.[3]

In the same way that in a binary polymer–solvent system the interaction parameter g constitutes the complete thermodynamic description of the system and predicting g is the test for any theoretical model, so in a ternary system the ternary parameter can be viewed as describing the characteristics of the system and being the goal for any interpretation of it.

However, a correct unequivocal determination of the ternary parameter has not been possible up to now, due to the lack of g data for the binary systems.

The case of infinite dilution of the polymer is the one for which total and preferential sorption have been most extensively studied. In this dilute solution limit the interpretation of the preferential adsorption coefficient, λ, requires knowledge of the g interaction parameters at infinite dilution, $g°$, for the polymer in each one of the pure liquids, according to the following expression:[4]

$$\lambda = -v_3° u_{10} u_{20} [l - 1 + g_{13}° - l g_{23}° + (u_{10} - u_{20})(g_{12} - g_T) - u_{10} u_{20} [\partial(g_{12} - g_T)/\partial u_1]°] / [u_{20} + l u_{10} - u_{10} u_{20} [2 g_{12} + 2(u_{10} - u_{20})(\mathrm{d}g_{12}/\mathrm{d}u_{10}) - u_{10} u_{20} (\mathrm{d}^2 g_{12}/\mathrm{d}^2 u_{10})]] \quad (1)$$

where u_1 is volume fraction of liquid 1 in the 1 + 2 liquid mixture ($u_1 + u_2 = 1$), zero denotes the limit of zero polymer concentration, $g_{13}°$ and $g_{23}°$ are the solvent 1–polymer and solvent 2–polymer g interaction parameters, g_{12} is the interaction parameter for the liquid mixture, $v_3°$ is polymer partial specific volume, and $l = V_1/V_2$ is the ratio of solvent molar volumes.

The lack of knowledge of $g°$ parameter values has led to different approximations, the crudest of them[2,3] being to substitute these parameters for their corresponding $\chi°$'s, which implies the assumption that polymer–solvent interaction parameters are not dependent on polymer concentration, in clear contradiction with overwhelming experimental evidence on the contrary.[5] To avoid such an approximation, it has been proposed to use the difference $g_{13}° - l g_{23}°$ as adjustable from the preferential adsorption data[4,6,7] jointly with the ternary parameter g_T.

However, for those binary polymer–solvent systems in which data of χ as a function of concentration are available, it is possible to obtain the g interaction parameters directly, as we shall explain below. With the g's thus determined, it should be unnecessary to use any approximation or adjustment of binary parameters in the study of ternary systems.

A similar case is the interpretation of gel permeation chromatography experiments through thermodynamic theories, according to which[8] the partition coefficient of the eluting polymer between gel and solvent phases depends on the binary g interaction parameters of the polymer–solvent, gel–solvent, and polymer–gel pairs.

The objective of the present work is to provide values of $g°$ of binary polymer–solvent systems. These can be useful thermodynamic information for the study of the binary systems themselves and also a source of data needed in the study of ternary systems.

Theory

For binary polymer–solvent systems, the Gibbs mixing function, ΔG_M, can be written, without approximation, as the sum of a combinatorial term plus an interactional term

$$\Delta G_M/RT = n_1 \ln v_1 + n_2 \ln v_2 + n_1 v_2 g_v \quad (2)$$

0024-9297/86/2219-1478$01.50/0

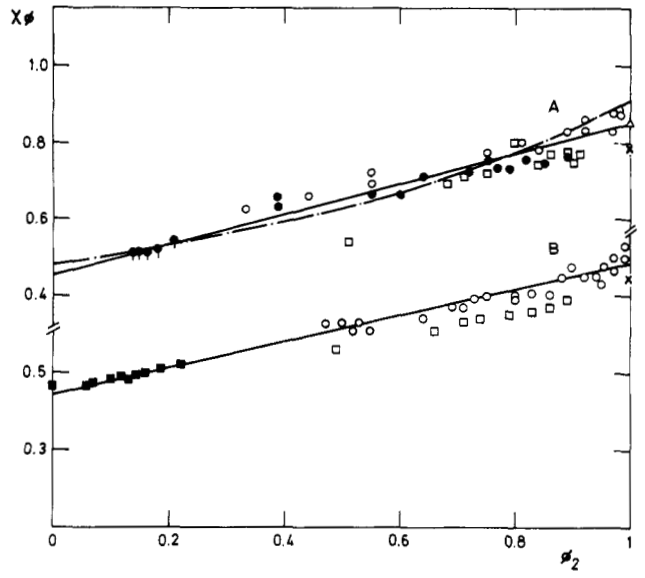

Figure 1. Plot of χ_ϕ against polymer segment fraction ϕ_2 for PDMS systems. (A) Benzene: (○) vapor pressure[14] (20 °C, $M = 5 \times 10^5$); (●, ⚲) vapor and osmotic pressure[15] (25 °C, $M = 5 \times 10^5$); (□) vapor pressure[16] (25 °C, $M = 4.2 \times 10^3$); (△) gas–liquid chromatography[17] (25 °C); (×) GLC[13] (25 °C, $M = 5 \times 10^5$). (B) Toluene: (○, □, ×) same as (A); (■) osmotic pressure[18] (20 °C, $M = 10^5$). (—) Drawn to fit the experimental points ((□) not considered). (-·-) Theoretical predictions[15] (25 °C).

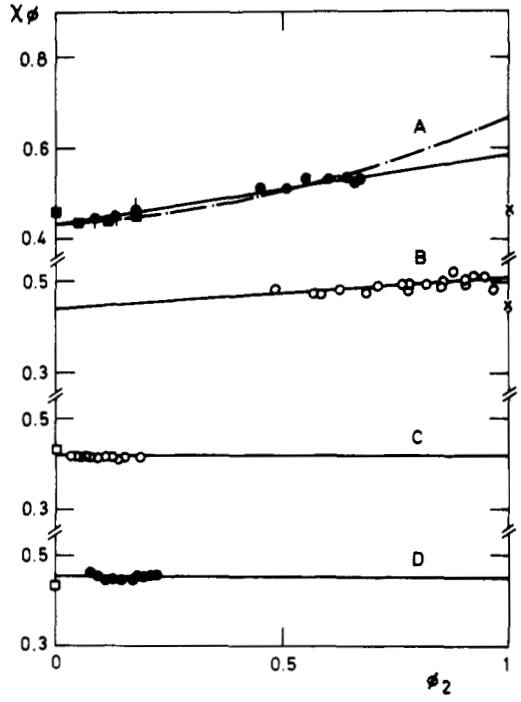

Figure 2. Plot of χ_ϕ against polymer segment fraction ϕ_2 for PDMS systems. (A) Cyclohexane: (■) osmotic pressure[18] (20 °C, $M = 10^5$); (●, ⚲) vapor and osmotic pressure[15] (25 °C, $M = 5 \times 10^5$); (×) GLC[13] (25 °C, $M = 5 \times 10^5$). (B) *n*-Pentane: (○) vapor pressure[14] (20 °C, $M = 5 \times 10^5$); (×) same as (A). (C and D) *n*-Hexane and *n*-nonane, respectively: (○, ●) osmotic pressure[19] (20 °C, $M = 1.4 \times 10^5$); (□) light scattering[20,21] (20 °C, $M = 1.2 \times 10^5$). (—) Drawn to fit the experimental points. (-·-) Theoretical predictions[15] (25 °C).

Here, n_i is amount of substance and v_i the volume fraction, this last magnitude being defined by $v_i = w_i v_{sp,i}/(w_1 v_{sp,1} + w_2 v_{sp,2})$, where w_i is the weight fraction and $v_{sp,i}$ the specific volume ($i = 1, 2$). Index 1 refers to solvent and index 2 to polymer. g is a phenomenological interaction parameter that takes into account deviations of ΔG_M from its combinatorial value. Subscript v in g_v denotes that g is defined on a volume fraction basis.

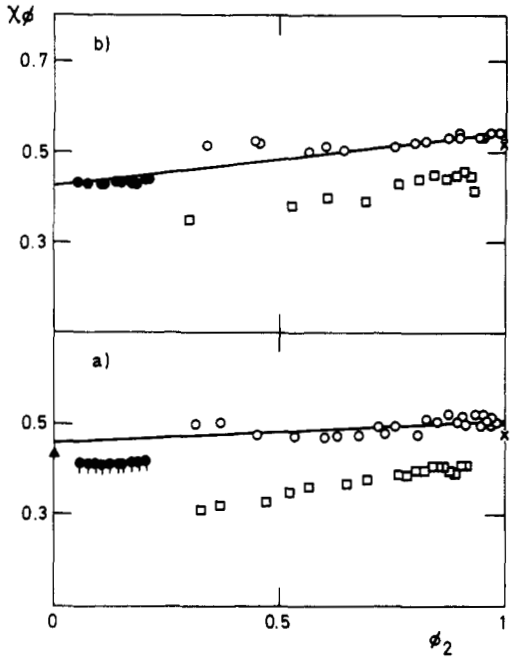

Figure 3. Plot of χ_ϕ against polymer segment fraction, ϕ_2, for PDMS systems. (a) *n*-Heptane: (○) vapor pressure[14] (20 °C, $M = 5 \times 10^5$); (□) vapor pressure[16] (25 °C, $M = 1.5 \times 10^3$); (⚲) osmotic pressure[19] (35 °C, $M = 1.4 \times 10^5$); (×) GLC[13] (25 °C, $M = 5 \times 10^5$); (▲) light scattering[20] (20 °C, $M = 1.2 \times 10^5$). (b) *n*-Octane: (○, □, and ×) same as (a); (●) osmotic pressure[19] (20 °C, $M = 1.4 \times 10^5$). (—) Drawn to fit the experimental points. ((□) not considered and (⚲) in 7a not considered).

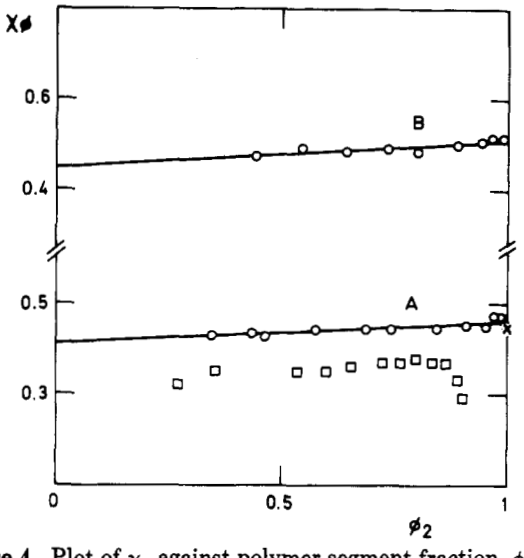

Figure 4. Plot of χ_ϕ against polymer segment fraction, ϕ_2, for PDMS systems. (A) 2,2,4-Trimethylpentane: (○) vapor pressure[14] (20 °C, $M = 5 \times 10^5$); (□) vapor pressure[16] (25 °C, $M = 4.2 \times 10^3$); (×) GLC[13] (25 °C, $M = 5 \times 10^5$). (B) 3-Methylheptane: (○) same as (A). (—) Drawn to fit the experimental points ((□) not considered).

Differentiating eq 2 gives the chemical potentials of the components: $\Delta\mu_1$ and $\Delta\mu_2$. For the solvent

$$\Delta\mu_1/RT = \ln v_1 + (1 - V_1/V_2)v_2 + v_2^2\chi_v \quad (3)$$

where

$$\chi_v = g_v + v_1(dg_v/dv_1) \quad (4)$$

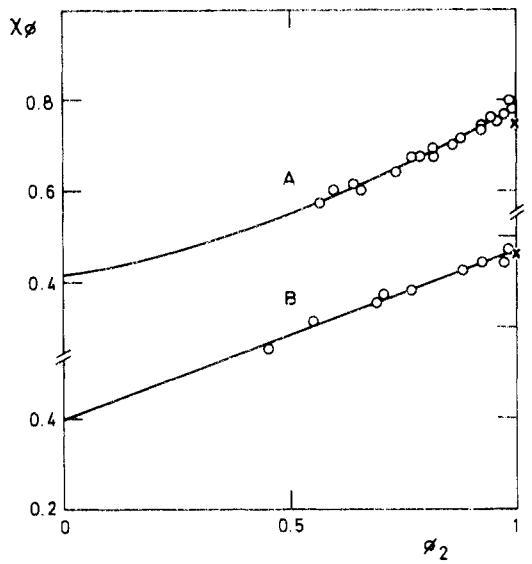

Figure 5. Plot of χ_ϕ against polymer segment fraction, ϕ_2, for PDMS systems. (A) *p*-Xylene: (O) vapor pressure[14] (20 °C, $M = 5 \times 10^5$); (×) GLC[13] (25 °C, $M = 5 \times 10^5$). (B) Ethylbenzene: (O) same as (A) at $T = 23.5$ °C; (×) same as (A). (—) Drawn to fit the experimental points.

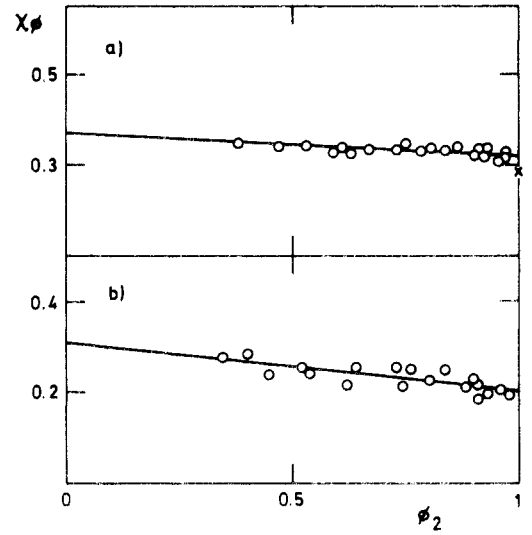

Figure 6. Plot of χ_ϕ against polymer segment fraction, ϕ_2, for PDMS systems. (a) Hexamethyldisiloxane: (O) vapor pressure[14] (20 °C, $M = 5 \times 10^5$); (×) GLC[13] (25 °C, $M = 5 \times 10^5$). (b) Octamethyltrisiloxane: (O) same as (a). (—) Drawn to fit the experimental points.

V_i being molar volume and χ a phenomenological interaction parameter taking into account the deviations of $\Delta\mu_1$ from its purely combinatorial value. Subscript v in χ_v denotes that χ is defined on a volume fraction basis (the same as g_v). This eq 3 would be not strictly applicable to the dilute solution limit, but it can be interpreted as the definition of χ for the whole range of concentrations.

If instead of volume fractions, segment fractions, ϕ_i, are used, then

$$\Delta G_M/RT = n_1 \ln \phi_1 + n_2 \ln \phi_2 + n_1\phi_2 g_\phi \quad (5)$$

with $\phi_i = w_i v^*_{sp,i}/(w_1 v^*_{sp,1} + w_2 v^*_{sp,2})$, where $v^*_{sp,i}$ is the characteristic (hard-core) specific volume ($i = 1, 2$). Differentiating eq 5 gives

$$\Delta\mu_1/RT = \ln \phi_1 + (1 - V_1^*/V_2^*)\phi_2 + \chi_\phi \phi_2^2 \quad (6)$$

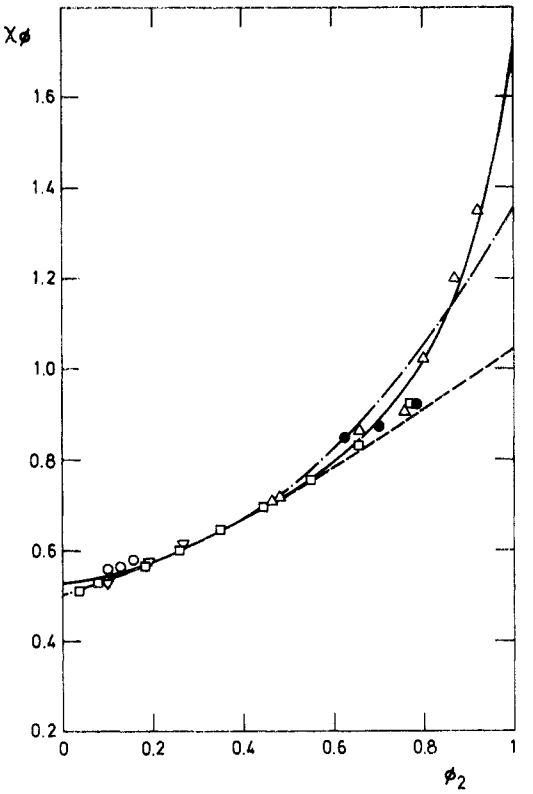

Figure 7. Plot of χ_ϕ against the polymer segment fraction, ϕ_2, for the cyclohexane–PS system: (O) osmotic pressure[22] (26 °C); (●) vapor pressure[23] (25 °C, $M = 15 \times 10^4$); (△) vapor pressure[24] (24 °C, $M = 26 \times 10^3$); (□) equilibrium ultracentrifugation[25] (30 °C, $M = 154 \times 10^3$); (---) critical miscibility[26] (25 °C, M = 35–1500 × 10^3); (▽) osmotic pressure[24] (24 °C, $M = 72 \times 10^3$). (—) Drawn to fit the experimental points. (-·-) Theoretical prediction[27] (25 °C).

where

$$\chi_\phi = g_\phi + \phi_1(dg_\phi/d\phi_1) \quad (7)$$

Subscript ϕ on interaction parameters g_ϕ and χ_ϕ means that g_ϕ and χ_ϕ are defined on a segment fraction basis, and V_i^* is the characteristic molar volume. These V_i^*'s are obtained from the reduced volumes, $\tilde{V}_i$

$$\tilde{V}_i = V_i/V_i^* \quad (8)$$

To obtain the reduced volumes, it is usual to use the equation of state due to Flory,[9] from which is derived[9]

$$\tilde{V}_i = [1 + \alpha_i T/3(1 + \alpha_i T)]^3 \quad (9)$$

α_i being the thermal expansion coefficient.

For the polymer component, differentiation of eq 2 gives a result similar to eq 3.

$$\Delta\mu_2/RT = \ln v_2 + (1 - V_2/V_1)v_1 + (V_2/V_1)v_1^2\chi_v' \quad (10)$$

where

$$\chi_v' = g_v + v_2(dg_v/dv_2) \quad (11)$$

χ_v' being a phenomenological interaction parameter for the noncombinatorial part of the solute (polymer) chemical potential, defined on a volume fraction basis. Equations similar to eq 10 and 11 serve to define χ' on a segment fraction basis, χ_ϕ'.

The relationship between the g parameters and the χ or χ' parameters is given by eq 4, 7, and 11. Integration of these equations up to the concentration v_2 (=1 − v_1) or ϕ_2 (=1 − ϕ_1) yields the value of g: g_v as a function of v_2 or g_ϕ as a function of ϕ_2. With the common symbol x to

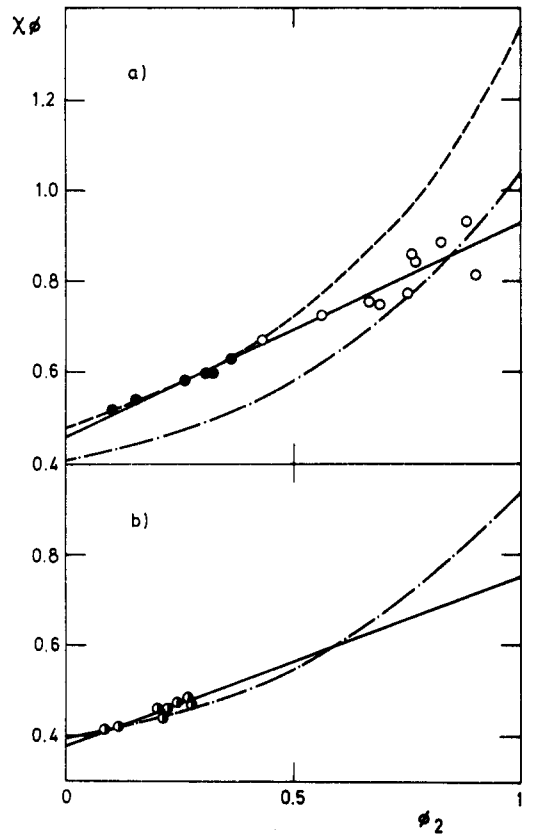

Figure 8. Plot of χ_ϕ against the polymer segment fraction, ϕ_2, for PS systems. (a) Methyl ethyl ketone: (○) vapor pressure[29] (25 °C, $M = 29 \times 10^4$); (●) osmotic pressure[28] (10, 50 °C, $M = 97 \times 10^3$). (—) Drawn to fit the experimental points; (-·-) and (---) theoretical prediction[28] (25 °C). (b) Ethylbenzene: (◑) osmotic pressure[30] (10, 35 °C, $M = 51 \times 10^3$). (—) Drawn to fit the experimental points; (-·-) theoretical prediction[30] (25 °C).

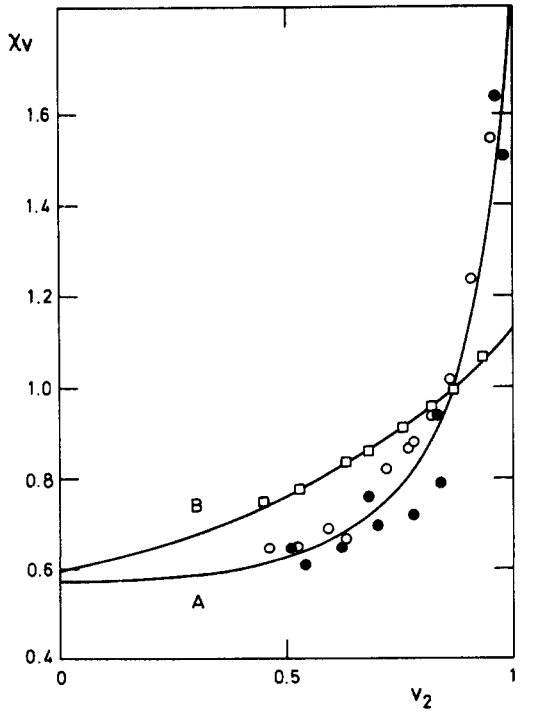

Figure 9. Plot of χ_v against the polymer volume fraction, v_2, for PS systems. (A) Diethyl ketone: (○, ●) vapor pressure[32] (20 °C, $M = 2 \times 10^5$ and 5×10^5). (B) Acetone: (□) vapor pressure[31] (25 °C, $M = 16 \times 10^3$). (—) Drawn to fit the experimental points.

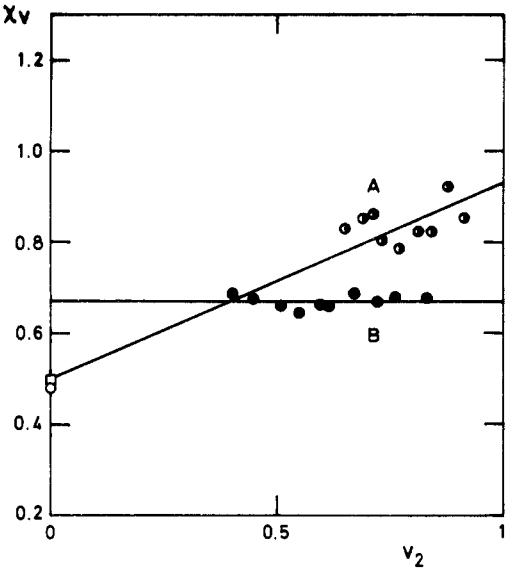

Figure 10. Plot of χ_v against the polymer volume fraction, v_2, for PS systems. (A) *n*-Butyl acetate: (◑) vapor pressure[32] (20 °C, $M = 5 \times 10^5$); (○) osmotic pressure[33] (30 °C, $M = 4 \times 10^5$). (B) *n*-Propyl acetate: (●) vapor pressure[31] (25 °C, $M = 2 \times 10^5$). Ethyl acetate: (□) osmotic pressure[34] (25 °C, $M = 24 \times 10^4$). (—) Drawn to fit the experimental points.

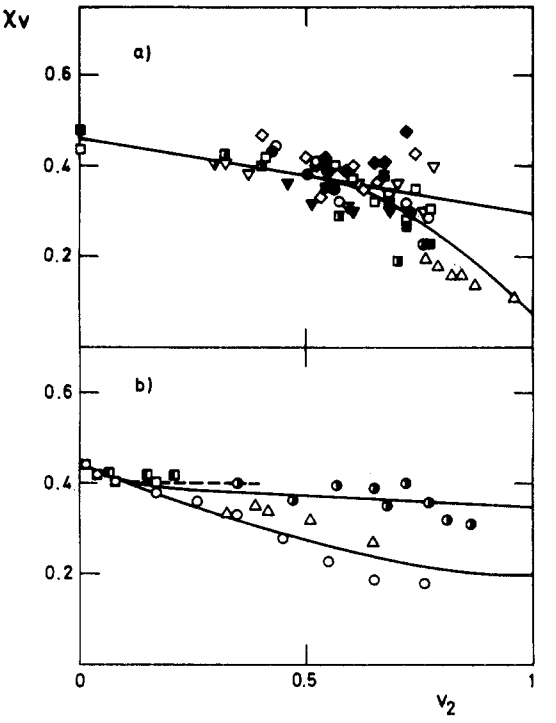

Figure 11. Plot of χ_v against the polymer volume fraction, v_2, for PS systems. (a) Benzene: (○, ◑, □, ◧, ▽, ▼) osmotic pressure[35] (15, 30, 45 °C, $M = 6.3 \times 10^4$, 90×10^4); (△) vapor pressure[36] (30 °C); (◇, ◆) vapor pressure[32] (20 °C, $M = 2 \times 10^4$, 5×10^5). (b) Toluene: (◑) vapor pressure[29] (25 °C, $M = 29 \times 10^4$); (△) osmotic pressure[35] (30 °C, $M = 9 \times 10^4$); (○) sedimentation equilibrium[37] (25 °C, $M = 15 \times 10^4$); (□) light scattering[38] (25 °C, $M = 52 \times 10^4$); (◧) osmotic pressure[39] (25 °C, $M = 2 \times 10^5$). (---) Small-angle X-ray scattering[40] (25 °C, $M = 4 \times 10^4$); (—) drawn to fit the experimental points.

represent either v or ϕ, the results are

$$g_x = \frac{1}{x_1}\int_0^{x_1} \chi \, dx_1 = \frac{1}{x_2}\int_0^{x_2} \chi' \, dx_2 \qquad (12)$$

($x = v$ or ϕ). In the limit of zero concentration of polymer

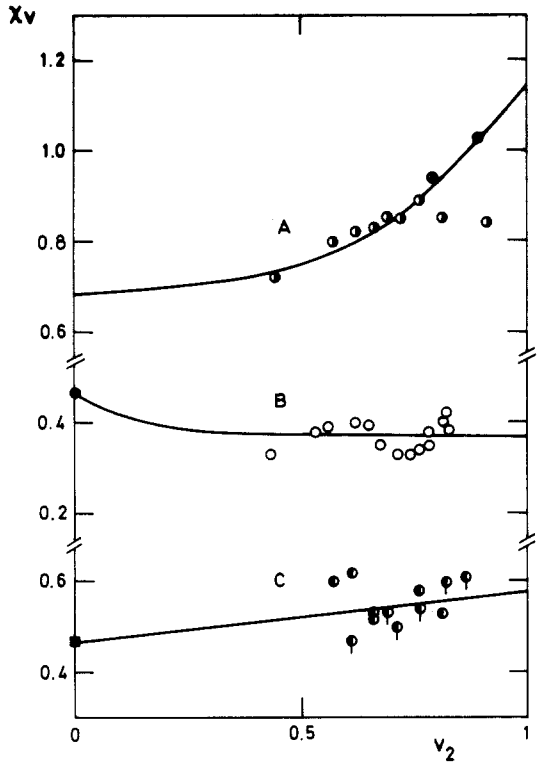

Figure 12. Plot of χ_v against the polymer volume fractions, v_2, for PS systems. (A) *n*-Propyl ether: (◑) vapor pressure[32] (20 °C, $M = 5 \times 10^5$). (B) Carbon tetrachloride: (○) vapor pressure[32] (20 °C, $M = 5 \times 10^5$); (●) osmotic pressure.[32] (C) Dioxane: (◐, ♀) vapor pressure[32] (20 °C, $M = 5 \times 10^5$, 2×10^3); (■) osmotic pressure.[32] (—) Drawn to fit the experimental points.

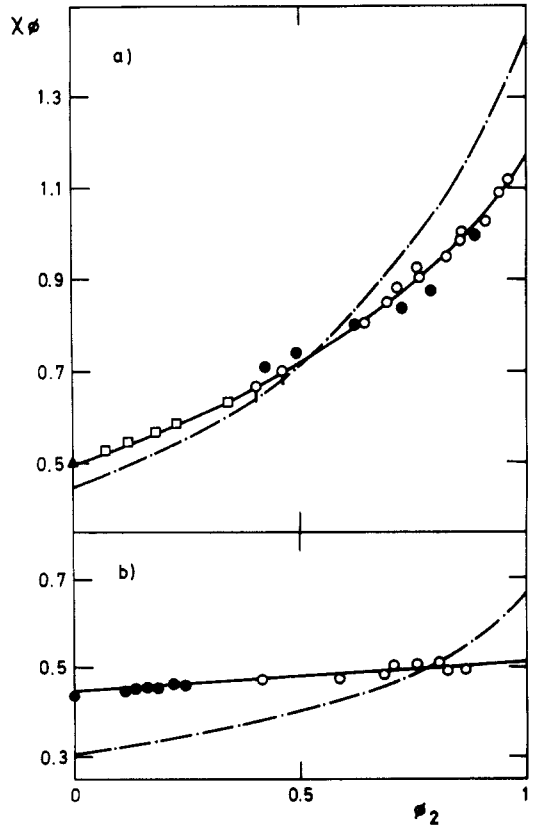

Figure 13. Plot of χ_ϕ against polymer segment fraction, ϕ_2, for PIB systems. (a) Benzene: (○, ♀) vapor and osmotic pressure[42] (25 °C, $M = 4 \times 10^4$); (□) vapor pressure[43] (24.5 °C); (●) vapor pressure[44] (25 °C, $M = 4.5 \times 10^4$); (▲) light scattering[45] (24–30 °C, $M = 1.3 \times 10^6$). (b) Cyclohexane: (○) vapor pressure[46] (25 °C, $M = 4 \times 10^4$); (●) vapor pressure[47,43] (30 °C). (—) Drawn to fit the experimental points; (-·-) theoretical predictions, ref 42 and 46, part (a) and (b), respectively, at 25 °C.

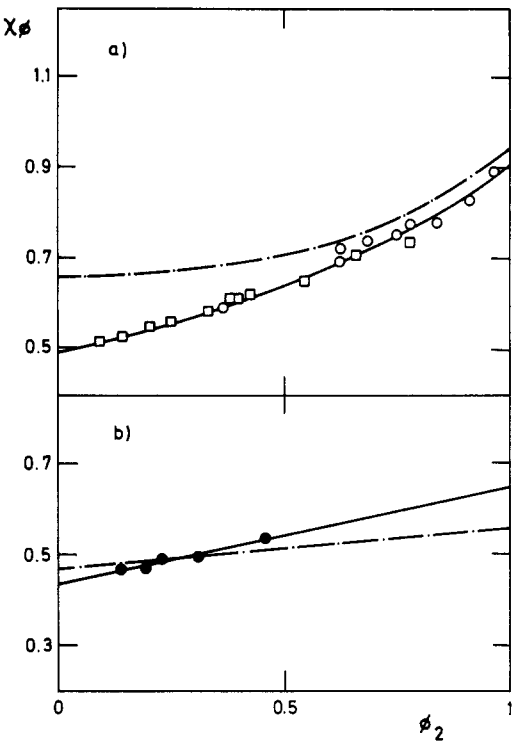

Figure 14. Plot of χ_ϕ against polymer segment fraction, ϕ_2, for PIB systems. (a) *n*-Pentane: (○) vapor pressure[48] (25 °C, $M = 4 \times 10^4$); (□) vapor pressure[43] (24.5 °C). (b) *n*-Octane: (●) osmotic pressure[49] (25 °C, $M = 4 \times 10^4$). (—) Drawn to fit the experimental points; (-·-) theoretical predictions, ref 48 and 50, part (a) and (b), respectively, at 25 °C.

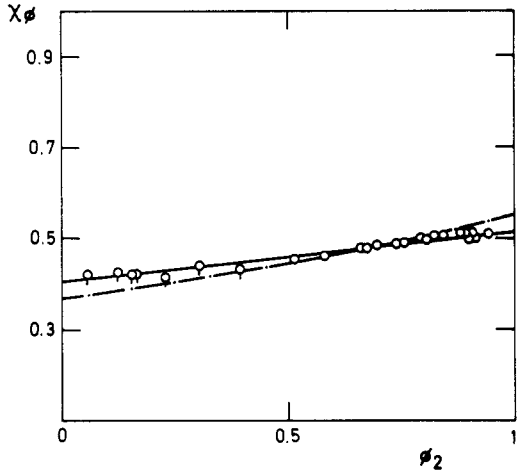

Figure 15. Plot of χ_ϕ against polymer segment fraction, ϕ_2, for benzene–NR system: (○, ♀) vapor and osmotic pressure[11] (25 °C, $M = 4 \times 10^4$). (—) Drawn to fit experimental points; (-·-) theoretical predictions[11] (25 °C).

($v_2 = \phi_2 = 0$) and in the limit of pure polymer ($v_2 = \phi_2 = 1$) we have

$$g_x^0 = \chi_x'^0 = \int_0^1 \chi \, dx_1 \tag{13}$$

$$g_x^1 = \chi_x^1 = \int_0^1 \chi' \, dx_2 \tag{14}$$

where the superscripts 0 and 1 mean respectively $v_2 = \phi_2 = 0$ and $v_2 = \phi_2 = 1$.

Equations 13 and 14 show that the g interaction parameter is the reduced residual chemical potential (a) of the polymer, in the limit $\phi_2 = 0$, and (b) of the solvent, in the limit $\phi_2 = 1$.

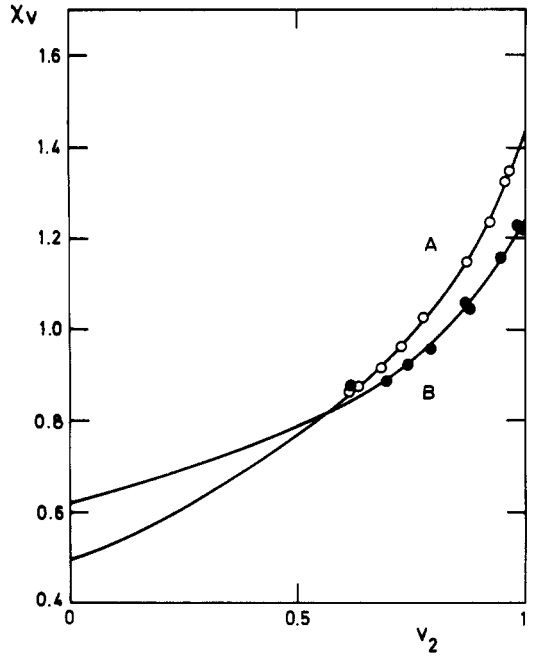

Figure 16. Plot of χ_v against polymer volume fraction, v_2, for NR systems. (A) Methyl ethyl ketone: (O) vapor pressure[50] (25 °C). (B) Ethyl acetate: (●) vapor pressure[50] (25 °C).

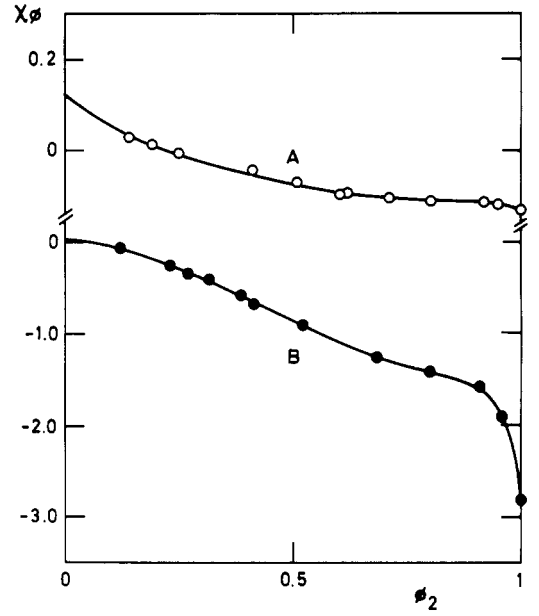

Figure 17. Plot of χ_ϕ against the polymer segment fraction, ϕ_2, for PPO systems. (A) Carbon tetrachloride: (O) vapor pressure[51] (5.5 °C, $M = 2 \times 10^3$). (B) Chloroform: (●) vapor pressure[51] (5.5 °C, $M = 2 \times 10^3$). (—) Drawn to fit the experimental points.

Determining $g°$

The empirical value of $g°$ can be obtained from the experimental result of the χ parameter (measured through the activity of the solvent) by means of eq 13

$$g_v° = \int_0^1 \chi_v \, dv_2 \tag{15}$$

$$g_\phi° = \int_0^1 \chi_\phi \, d\phi_2 \tag{16}$$

These two $g°$ parameters are related, so that knowledge of χ in both scales of concentration and integration over the two variables (v_2 and ϕ_2) is not needed. If χ is known in one of the scales and $g°$ is calculated by integration over one of the variables, then the other $g°$ can be obtained by knowing the reduced volumes of the polymer and solvent. According to eq 3, 6, 15, and 16 it is

$$g_\phi° = \int_0^1 [v_2^2\chi_v + \ln(v_1/\phi_1) + v_2 - \phi_2 - (v_2V_1/V_2 - \phi_2V_1^*/V_2^*)]\phi_2^{-2} \, d\phi_2 \tag{17}$$

Using the change of variables $v_2 = \phi_2(\tilde{V}_2/\tilde{V}_1)[1 - \phi_2(1 -$

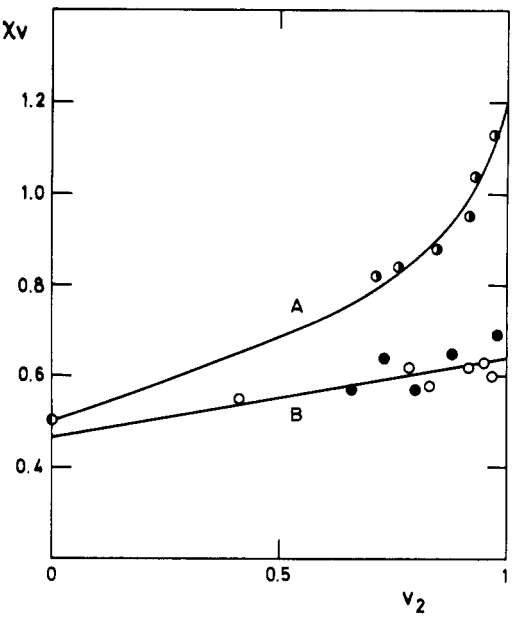

Figure 18. Plot of χ_v against the polymer volume fraction, v_2, for POCS systems. (A) Methyl ethyl ketone: (◑) vapor pressure[52] (25 °C, $M = 60 \times 10^4$); (◐) light scattering[53] (25 °C). (B) Benzene: (●, O) vapor pressure[52] (25, 40 °C, $M = 60 \times 10^4$). (—) Drawn to fit experimental points.

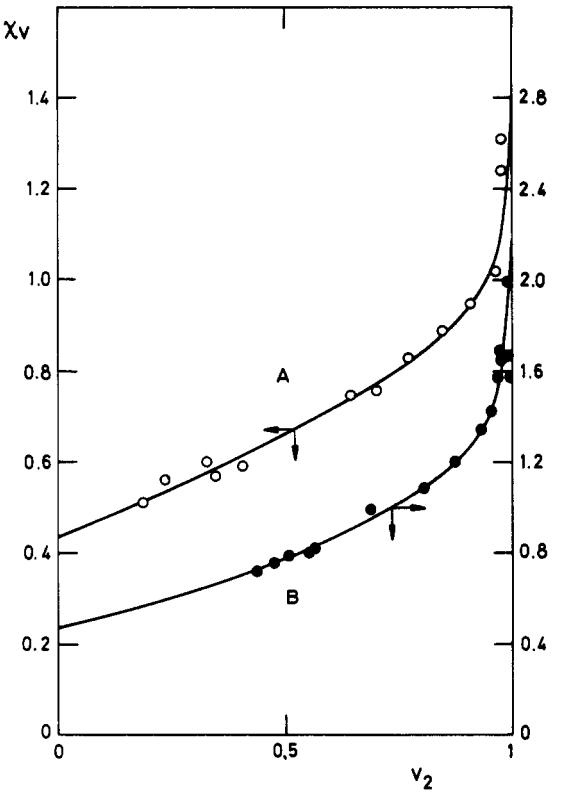

Figure 19. Plot of χ_v against polymer volume fraction, v_2, for PP systems. (A) Diisobutyl ketone: (O) vapor pressure[54] (25 °C, $M = 2 \times 10^4$). (B) Diethyl ketone: (●) vapor pressure[54] (25 °C, $M = 2 \times 10^4$). (—) Drawn to fit experimental points.

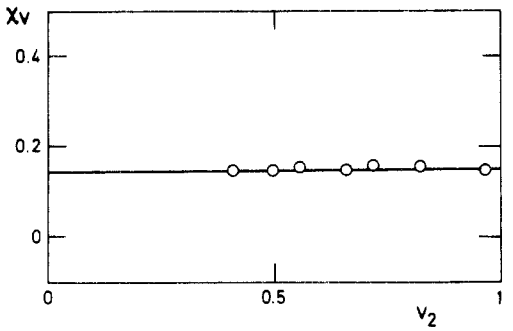

Figure 20. Plot of χ_v against polymer volume fraction, v_2, for the chloroform–PBD system: (O) vapor pressure[55] (25 °C). (—) Drawn to fit experimental points.

Table I
Polymers Studied in Figures 1–20

polymer	abbrev	figures
poly(dimethylsiloxane)	PDMS	1–6
polystyrene	PS	7–12
polyisobutylene	PIB	13, 14
natural rubber	NR	15, 16
poly(propylene oxide)	PPO	17
poly(*o*-chlorostyrene)	POCS	18
polypropylene	PP	19
polybutadiene	PBD	20

$\tilde{V}_2/\tilde{V}_1)]$ and performing the integration, we get

$$g_\phi^\circ = g_v^\circ \tilde{V}_2/\tilde{V}_1 + 1 - (\tilde{V}_2/\tilde{V}_1)[1 - (V_1/V_2)\ln(\tilde{V}_2/\tilde{V}_1)] \quad (18)$$

This equation allows us to calculate g_ϕ° from g_v° or vice versa. For long chains ($V_1/V_2 \to 0$), eq 18 reduces to

$$g_\phi^\circ = g_v^\circ \tilde{V}_2/\tilde{V}_1 + 1 - \tilde{V}_2/\tilde{V}_1 \quad (19)$$

Theoretical g°

The theoretical expression for the g° parameter, using the theory of polymer solutions developed by Flory and by Patterson based on the ideas of Prigogine and his school, has been recently given by Horta.[10] With the equivalences of the Flory theory for the reduced configurational energy, $\tilde{U}$, and entropy, $\tilde{S}$, namely, $\tilde{U} = -\tilde{V}^{-1}$ and $\tilde{S} = 3\ln(\tilde{V}^{1/3} - 1)$, and the use of eq 18, the expression for g° of ref 10 can be written

$$g_\phi^\circ = \frac{p_1^* V_1^*}{RT}\left\{\frac{p_2^*}{p_1^*}\left[\frac{1}{\tilde{V}_2} - \frac{1}{\tilde{V}_1} - \frac{T}{T_2^*}3\ln\left(\frac{\tilde{V}_1^{1/3} - 1}{\tilde{V}_2^{1/3} - 1}\right)\right] + \frac{s_2/s_1}{\tilde{V}_1}\frac{\bar{X}_{12}}{p_1^*}\right\} \quad (20)$$

where p_i^* and T_i^* are characteristic (reduction) parameters for pressure and temperature, s_i is the number of contact sites per segment, and $\bar{X}_{12} = X_{12} - \tilde{V}_1 T Q_{12}$, with X_{12} and Q_{12} representing the exchange energy and entropy, respectively, for the formation of 1–2 contacts per unit core volume.

The parameter g° can thus be calculated theoretically by means of eq 20 and this theoretical g° be compared with the empirical g° (determined from the experimental χ through eq 16), if the values of s_2/s_1, X_{12}, and Q_{12} are known for the system. For some of the systems studied in the present work, the values of s_2/s_1, X_{12}, and Q_{12} are available in the literature. They have been determined by fitting the theoretical χ_ϕ vs. ϕ_2 variation to experiment, using for χ_ϕ the expression of the Flory theory[11]

Table II
Empirical Values of the g Interaction Parameters at Infinite Dilution Calculated from the Experimental Data of χ vs. Polymer Concentration According to Eq 15, 16, and 19

system[a]	T, °C	$\tilde{V}_2/\tilde{V}_1$	g_ϕ°	g_v°
PDMS–benzene	20, 25	0.9509[b]	0.65	0.63
PDMS–toluene†	20	0.9722	0.61	0.60
PDMS–cyclohexane†	20, 25	0.9517[b]	0.51	0.49
PDMS–*n*-pentane	20	0.9099	0.47	0.42
PDMS–*n*-hexane	20	0.9324	0.42	0.38
PDMS–*n*-heptane	20	0.9509	0.46	0.43
PDMS–*n*-octane†	20	0.9619	0.49	0.47
PDMS–*n*-nonane	20	0.9712	0.45	0.43
PDMS–2-2-4-trimethylpentane	20	0.9595	0.44	0.42
PDMS–3-methylpentane	20	0.9996	0.48	0.48
PDMS–*p*-xylene	20	0.9823	0.55	0.54
PDMS–ethylbenzene	20	0.9828	0.58	0.57
PDMS–hexamethyldisiloxane	20	0.9303	0.34	0.29
PDMS–octamethyltrisiloxane	20	0.9487	0.26	0.22
PS–cyclohexane†	20–30	0.8932[b]	0.84	0.82
	25		0.74	0.71[c]
PS–methyl ethyl ketone†	10, 25, 50	0.8817[b]	0.70	0.65
PS–ethylbenzene	10, 35	0.9211[b]	0.56	0.53
PS–diethyl ketone	20	0.8995	0.78	0.75
PS–acetone	25	0.8705	0.82	0.79
PS–*n*-propyl acetate	25	0.8813	0.71	0.67
PS–*n*-butyl acetate	20	0.9036	0.71	0.68
PS–benzene	15–45	0.8719[d]	0.42	0.34
			0.46	0.38
PS–toluene	25,30	0.9221[b]	0.35	0.29
			0.42	0.37
PS–*n*-propyl ether	20	0.8904	0.82	0.80
PS–carbon tetrachloride	20	0.8891	0.45	0.38
PS–dioxane	20	0.9131	0.56	0.52
PIB–benzene†	25	0.8894	0.73	0.70
PIB–*n*-pentane†	25	0.8443	0.66	0.60
PIB–*n*-octane	25	0.8980	0.54	0.49
PIB–cyclohexane†	25	0.8901	0.48	0.42
NR–benzene†	25	0.9075	0.46	0.40
NR–methyl ethyl ketone	25	0.8965	0.83	0.81
NR–ethyl acetate	25	0.8924	0.84	0.82
PPO–carbon tetrachloride†	5.6	0.9391	−0.05	−0.12
PPO–chloroform†	5.6	0.9272	−0.86	−1.01
POCS–benzene	25, 40			0.55
POCS–methyl ethyl ketone	25			0.73
PP–diethyl ketone	25		0.85	
PP–diisobutyl ketone	25		0.70	
PBD–chloroform†	25		0.15	

[a] Dagger indicates data available on the whole concentration range. [b] At 25 °C. [c] Reference 26. [d] At 30 °C.

$$\chi_\phi = \frac{p_1^* V_1^*}{RT}\left[\frac{1}{\tilde{V}_1} - \frac{1}{\tilde{V}} + \frac{T}{T_1^*}3\ln\left(\frac{\tilde{V}_1^{1/3} - 1}{\tilde{V}^{1/3} - 1}\right) + \frac{X_{12} - \tilde{V}TQ_{12}}{p_1^*}\frac{\theta_2^2}{\tilde{V}}\right]\phi_2^{-2} \quad (21)$$

where $\theta_2 = \phi_2[(s_1/s_2)\phi_1 + \phi_2]^{-1}$, and $\tilde{V}$ is the reduced volume of the system.

Systems

To calculate g° through eq 15 and 16 we have taken from the literature data of χ as a function of concentration. Due to the variety of sources for the several systems studied, the data correspond to different polymer molecular weights, M, and to different temperatures. Since the variation of χ with concentration may depend on M for low M's, we have selected data only for $M \gtrsim 2 \times 10^4$,[12] where no M dependence is detected. The temperatures have been chosen close to 25 °C as the most useful T for

Table III
Literature Values of X_{12}, Q_{12}, and s_1/s_2 and Values of the Interaction Parameter, $g_\phi°$, Calculated from Expression 20 Using These Parameters

system[a]	X_{12}, cal cm^{-3}	Q_{12}, cal cm^{-3} deg^{-1}	s_1/s_2	ref	$g_\phi°$
PDMS–benzene†	9.12	0	1.32	15	0.651
PDMS–cyclohexane†	5.52	0	1.2	15	0.516
PIB–*n*-pentane	2.8	0	1.89	49	0.745
PIB–benzene	10	0	1.72	42	0.796
PIB–cyclohexane	1.4	0	1.61	46	0.420
PIB–*n*-octane	1.05	0	1.72	50	0.537
NR–benzene†	1.40	−0.0044	1.11	11	0.451
PS–cyclohexane†	10.03	0.0055	2.0	27	0.81
PS–methyl ethyl ketone	6.21	0	2.08	28	0.62
PS–methyl ethyl ketone	6.21	−0.0091	2.08	28	0.77
PS–ethylbenzene	2.10	−0.0069	1.89	30	0.58

[a] Dagger indicates the theoretical values of $g_\phi°$ are in agreement with the experimental values.

application of the calculated $g°$'s. In some systems the temperature dependence of the χ vs. concentration variation is unnoticeable, and it has been possible to combine results at different T's (close to 25 °C) in order to extend the range of concentration covered by the data.

In general, the data selected from the literature have been determined by a variety of experimental techniques, each one operating within a range of accessible concentrations: light scattering (dilute solution), osmotic pressure (concentrations up to 30%), solvent vapor pressure (extended range reaching 90%), critical miscibility, sedimentation equilibrium, and inverse gas chromatography ($v_2 \to 1$, although values of χ determined by this last technique have been found to be lower than those obtained extrapolating to $v_2 \to 1$ the χ's determined by static methods[13]). For a given system, we have combined the data determined by the different techniques in order to cover the v_2 = 0–1 range as fully as possible.

The error margin in the calculated $g°$ depends on the accuracy and precision of the experimental χ's and also on the portion of the v_2 = 0–1 range that is sampled by the χ data in each system. For this reason, we have chosen primarily systems whose χ is known over a wide enough range of v_2 and whose results from different authors, when available, are in reasonable agreement. However, other systems whose χ are known only over a limited range of v_2 but can be extrapolated without much uncertainty have been chosen also. In these latter systems, the calculation of $g°$ carries a larger error. The systems that are better determined, because their χ's are known in the whole v_2 = 0–1 range, are marked with a dagger in Table II.

A total of 41 polymer–solvent systems have been studied. They are represented in Figures 1–20 and correspond to the polymers listed in Table I. All the information concerning the experimental χ's of each system and the references to the original data are specified on the figure legends. In each system, a smooth curve has been drawn (continuous curves on the figures) to represent the variation of χ with concentration collectively determined by all the experimental data available for the system. (In two systems doubt arises, and two continuous curves have been drawn to represent the likely variation of experimental χ (PS–benzene and PS–toluene).)

Graphical integration of this experimental (continuous) curve has been used to obtain $g°$ according to eq 15 and 16. In those systems whose χ vs. v_2 or ϕ_2 variation is linear, the integration has been carried out analytically (instead of graphically), using the linear least-squares fit of the data. The experimental data are on the v_2 or on the ϕ_2 scales, depending on the system, thus yielding on integration g_v or g_ϕ, respectively. Interconversion between $g_v°$ and $g_\phi°$ for a given system has been achieved through eq 19 with the reduced volumes of polymer and solvent.

The values of $g°$ calculated for the 41 systems studied are collected in Table II. In those cases in which $\tilde{V}_2/\tilde{V}_1$ is known, both $g_v°$ and $g_\phi°$ are given. For the rest of the systems, only $g_v°$ is given.

The particular system PS + cyclohexane is the only one for which we have found in the literature a value of $g°$ calculated (by Koningsveld et al.[26]). This literature $g°$ is shown in Table II for comparison. It is obtained when the integral of eq 16 is performed by following the discontinuous curve of Figure 7. Such a curve is a theoretical extrapolation by Koningsveld et al.[26] of their experimental critical miscibility data, determined in the range $\phi_2 \leq 0.2$. The value of $g°$ calculated here for this system is higher because we have taken into account data of χ extending over a wider range of ϕ_2, which determine a steeper variation of χ at high ϕ_2 (the continuous curve of Figure 7).

$g°$ from Theoretical Parameters

The dash–dot curves drawn in Figures 1, 2, 7, 8, 13, 14, and 15 have been taken from the literature (see the figure legends) and represent the theoretical χ vs. ϕ_2 variation calculated with eq 21 for χ. Table III shows the values of the theoretical parameters s_1/s_2, X_{12}, and Q_{12} that correspond to such theoretical χ curves.

With these s_1/s_2, X_{12}, and Q_{12} parameters, we calculate $g°$ theoretically through eq 20, using the equation of state data for the pure components shown in Table IV. The results of the $g°$'s thus calculated theoretically are given in Table III (together with the parameter values used).

As we can see, the agreement between these $g°$'s calculated theoretically and the empirical ones of Table II is perfect in some systems (marked with a dagger in Table III). This agreement is to be expected since in these systems the values of s_1/s_2, X_{12}, and Q_{12} reproduce the experimental variation of χ with polymer concentration. However, in the other systems there are deviations, some of them very important. To achieve agreement in these latter cases would require modification of the theoretical

Table IV
Equation of State Data and Characteristic Parameters for Several Polymers and Solvents at 298.15 K

substance	v_{sp}, cm^3 g^{-1}	$\alpha \times 10^3$, deg^{-1}	$\tilde{V}$	v_{sp}*, cm^3 g^{-1}	T*, K	p*, cal cm^{-3}	ref
PDMS	1.0312	0.9068	1.2283	0.8395	5528	81.84	15
PIB	1.0906	0.555	1.1488	0.9493	7580	107	42
NR	1.0951	0.654	1.1722	0.9342	6775	124	11
PS	0.9336	0.572	1.1528	0.8098	7420	131	27
benzene	1.0312	0.9068	1.2917	0.8860	4709	150	15
cyclohexane	1.2922	1.217	1.2906	1.0012	4721	127, 2	15
n-pentane	1.6094	1.61	1.3607	1.1828	4158	97.1	14
n-octane	1.4320	1.159	1.2793	1.1194	4836	103.5	14
methyl ethyl ketone	1.2502	1.308	1.3075	0.9561	4557	139	28
ethylbenzene	1.1592	1.019	1.2515	0.9262	5176	132	14

s_1/s_2, X_{12}, and Q_{12} parameter values proposed in the literature.

Acknowledgment. Grateful thanks are extended to Dr González Rubio for this continued cooperation in this work. This work has received financial support from CAICYT, Ministerio de Educación y Ciencia, Spain, under Grant No. 0933/81.

References and Notes

(1) Flory, P. J. *Principles of Polymer Chemistry*, Cornell University: Ithaca, NY, 1953.
(2) Read, B. E. *Trans. Faraday Soc.* **1960**, *56*, 382.
(3) Gargallo, L.; Radic, D. *Adv. Colloid Interface Sci.* **1984**, *21*, 1.
(4) Pouchlý, J.; Zivný, A. *Makromol. Chem.* **1982**, *183*, 3019.
(5) Flory, P. J. *J. Chem. Soc., Faraday Discuss.* **1970**, *49*, 7.
(6) Chu, S. G.; Munk, P. *Macromolecules* **1978**, *11*, 879.
(7) Figueruelo, J. E.; Celda, B.; Campos, A. *Macromolecules* **1985**, *18*, 7511.
(8) Barrales, J. M.; Galera Gómez, P. A.; Horta, A.; Saiz, E. *Macromolecules* **1985**, *18*, 2572.
(9) Flory, P. J. *J. Am. Chem. Soc.* **1965**, *87*, 1833.
(10) Horta, A. *Macromolecules* **1985**, *18*, 2498.
(11) Eichinger, B. E.; Flory, P. J. *Trans. Faraday Soc.* **1968**, *64*, 2035.
(12) Except for the systems: acetone-PS, carbon tetrachloride-PPO and chloroform-PPO.
(13) Lichtenthaler, R. N.; Liu, D. D.; Prausnitz, J. M. *Ber. Bunsen-Ges. Phys. Chem.* **1984**, *78*, 470.
(14) Chahal, R. S.; Kao, W. P.; Patterson, D. *J. Chem. Soc., Faraday Trans. 1* **1973**, *69*, 1834.
(15) Flory, P. J.; Shih, H. *Macromolecules* **1972**, *5*, 761.
(16) Dolch, E.; Glaser, M.; Heintz, A.; Wagner, H.; Lichtenthaler, R. N. *Ber. Bunsen-Ges. Phys. Chem.* **1984**, *88*, 479.
(17) Summers, W. R.; Tewari, Y. B.; Schreiber, H. P. *Macromolecules* **1972**, *5*, 12.
(18) Kuwahara, N.; Okazawa, T.; Kaneko, M. *J. Polym. Sci.* **1968**, *23*, 513.
(19) Sugamiya, K.; Kuwahara, N.; Kaneko, M. *Macromolecules* **1974**, *7*, 66.
(20) Campos, A.; Celda, B.; Tejero, R.; Figueruelo, J. E. *Eur. Polym. J.* **1984**, *20*, 447.
(21) Celda, B., Ph. D. Thesis, Universidad de Valencia, Valencia, Spain, 1984.
(22) Palmen, H. J.; Möller, D.; Wefers, W. Presented at IUPAC Symposium on Macromolecules, Toronto, Canada, Sep 1968.
(23) Schmoll, K.; Jenckel, E. *Z. Elektrochem.* **1956**, *60*, 756.
(24) Krigbaum, W. R.; Geymer, D. O. *J. Am. Chem. Soc.* **1959**, *81*, 1859.
(25) Scholte, G. *J. Polym. Sci., Part A-2*, **1970**, *8*, 841.
(26) Koningsveld, R.; Kleintjens, L. A.; Schultz, A. R. *J. Polym. Sci., Part A-2* **1970**, *8*, 1261.
(27) Höcker, H.; Shih, H.; Flory, P. J. *Trans. Faraday Soc.* **1971**, *67*, 2275.
(28) Flory, P. J.; Höcker, H. *Trans. Faraday Soc.* **1971**, *67*, 2258.
(29) Bawn, C. E. H.; Freeman, R. F. J.; Kamaliddin, A. R. *Trans. Faraday Soc.* **1950**, *46*, 677.
(30) Höcker, H.; Flory, P. J. *Trans. Faraday Soc.* **1971**, *67*, 2270.
(31) Bawn, C. E. H.; Wajid, M. A. *Trans. Faraday Soc.* **1956**, *52*, 1658.
(32) Baugham, E. C. *Trans. Faraday Soc.* **1948**, *44*, 495.
(33) Kubo, K.; Ogino, K. *Bull. Chem. Soc. Jpn.* **1971**, *44*, 997.
(34) Jacobsson, G. *Acta Chem. Scand.* **1954**, *8*, 1843. In Figure 10 the value of χ_v° at dilute solution from the extrapolation of the experimental points of χ_v vs. v_2 for the system PS–*n*-propyl acetate is larger than the values of χ_v° corresponding to the systems PS–ethyl acetate and PS–*n*-butyl acetate which are experimental. Such a higher value of the extrapolated χ_v° could be a consequence of the lack of experimental values of χ_v at lower polymer concentrations. Thus the value of g_v° obtained for the system PS–*n*-propyl acetate could be overestimated.
(35) Noda, I.; Higo, Y.; Ueno, N.; Fujimoto, T. *Macromolecules* **1984**, *17*, 1055.
(36) Riedl, B.; Prud'homme, E. *Polym. Eng. Sci.* **1984**, *24* (17), 1291; *Eng. Sci.* **1984**, *24* (17), 1291.
(37) Scholte, Th. G. *J. Polym. Sci., Part A-2* **1970**, *8*, 841.
(38) Scholte, Th. G. *Eur. Polym. J.* **1970**, *6*, 1063.
(39) Shiomi, T.; Kohno, K.; Yoneda, K.; Tomita, T.; Miya, M.; Imai, K. *Macromolecules* **1985**, *18*, 414.
(40) Kinugasa, S.; Hayashi, H.; Hamade, F.; Nakajima, A. *Macromolecules* **1985**, *18*, 582.
(41) Higo, Y.; Ueno, N.; Noda, I. *Polym. J. (Tokyo)* **1983**, *15*, 367.
(42) Eichinger, B. E.; Flory, P. J. *Trans. Faraday Soc.* **1968**, *64*, 2053.
(43) Flory, P. J.; Daoust, H. *J. Polym. Sci.* **1957**, *25*, 429.
(44) Bawm, E. H.; Patel, R. D. *Trans. Faraday Soc.* **1956**, *52*, 1664.
(45) Silverberg, A.; Eliassaff, J.; Katschalsky, A. K. *J. Polym. Sci.* **1957**, *23*, 259.
(46) Eichinger, B. E.; Flory, P. J. *Trans. Faraday Soc.* **1968**, *64*, 2061.
(47) Krigbaum, W. R.; Flory, P. J. *J. Am. Chem. Soc.* **1953**, *75*, 1775.
(48) Eichinger, B. E.; Flory, P. J. *Trans. Faraday Soc.* **1968**, *64*, 2066.
(49) Flory, P. J.; Ellenson, J. L.; Eichinger, B. E. *Macromolecules* **1968**, *1*, 279.
(50) Booth, C.; Gee, G.; Holden, G.; Williamson, G. R. *Polymer* **1964**, *5*, 343.
(51) Kershaw, R. W.; Malcolm, G. N. *Trans. Faraday Soc.* **1968**, *64*, 323.
(52) Gekko, K.; Matsumura, N. *Bull. Chem. Soc. Jpn.* **1973**, *46*, 1554.
(53) Matsumura, K. *Polym. J. (Tokyo)* **1970**, *1* (3), 322.
(54) Brown, W. B.; Gee, G.; Taylor, W. D. *Polymer* **1964**, *5*, 362.
(55) Booth, C.; Gee, G.; Jones, M. N.; Taylor, W. D. *Polymer* **1964**, *5*, 353.

Communications to the Editor

Influence of Stretched and Unstretched Low-Density Polyethylene on the Photochemistry of a Conformationally Labile Ketone Dopant[1]

A wide variety of order solvents have been employed to alter the thermal and photochemical reactivities of solutes.[2] Alternatively, careful analyses of phase-dependent changes in reaction selectivities can be used to characterize the microenvironments of solutes. In principle, the simpler the solvent system, the greater will be the potential for obtaining useful structural and dynamic information from solute reactions.

Long *n*-alkanes are recognized to be "simple" isotropic liquids which contain small domains of longitudinal alignment.[3] The fluxional behavior of these liquids and the weakness of the van der Waals forces responsible for their alignment have made the domains of little practical use.[4] We view low-density polyethylene (LDPE) as an extremely viscous hydrocarbon solvent in which alkyl chains experience extensive local, semipermanent ordering[5] much like that of nematic liquid-crystalline phases.[6] As such, it may allow the effect of solvent chain alignment on solute reactivity to be observed in ways which are unavailable to *n*-alkanes.

In spite of its potential, very few examples of LDPE as a reaction medium have appeared. The photodimerization of tetraphenylbutatriene[7a] and the Norrish II reactions of 2-alkanones[7b] are the only examples of which we are aware. The first reaction is the sole example in which a comparison between reactivity in stretched and unstretched LDPE has been made. A threefold increase in quantum

0024-9297/86/2219-1486$01.50/0